Journal of Lasers in Medical Sciences

J Lasers Med Sci 2022;13:e35

Original Article

http://journals.sbmu.ac.ir/jlms

doi 10.34172/jlms.2022.35

Investigation into Chronic Low-Dose Ionizing Radiation Effect on Gene Expression Profile of Human HUVECs Cells

Mojtaba Ansari[1], Mostafa Rezaei-Tavirani[2*], Maryam Hamzeloo-Moghadam[3], Mohhamadreza Razzaghi[4], Babak Arjmand[5], Mona Zamanian Azodi[6], Mahmood Khodadoost[3], Farshad Okhovatian[7]

[1]Faculty of Medicine, Imam Hosein Hospital, Shahid Beheshti University of Medical Sciences, Tehran, Iran
[2]Proteomics Research Center, Faculty of Paramedical Sciences, Shahid Beheshti University of Medical Sciences, Tehran, Iran
[3]Traditional Medicine and Materia Medica Research Center, Department of Traditional Pharmacy, School of Traditional Medicine, Shahid Beheshti University of Medical Sciences, Tehran, Iran
[4]Laser Application in Medical Sciences Research Center, Shahid Beheshti University of Medical Sciences, Tehran, Iran
[5]Cell Therapy and Regenerative Medicine Research Center, Endocrinology and Metabolism Molecular-Cellular Sciences Institute, Tehran University of Medical Sciences, Tehran, Iran
[6]Proteomics Research Center, Shahid Beheshti University of Medical Sciences, Tehran, Iran
[7]Physiotherapy Research Center, Shahid Beheshti University of Medical Sciences, Tehran, Iran

***Correspondence to**
Mostafa Rezaei-Tavirani,
Email: tavirany@yahoo.com

Received: May 21, 2022
Accepted: July 19, 2022
Published online August 27, 2022

Abstract

Introduction: Understanding the molecular mechanism of chronic low-dose ionizing radiation (LDIR) effects on the human body is the subject of many research studies. Several aspects of cell function such as cell proliferation, apoptosis, inflammation, and tumorigenesis are affected by LDIR. Detection of the main biological process that is targeted by LIDR via network analysis is the main aim of this study.

Methods: GSE66720 consisting of gene expression profiles of human umbilical vein endothelial cells (HUVECs) (a suitable cell line to be investigated), including irradiated and control cells, was downloaded from Gene Expression Omnibus (GEO). The significant differentially expressed genes (DEGs) were determined and analyzed via protein-protein interaction (PPI) network analysis to find the central individuals. The main cell function which was related to the central nodes was introduced.

Results: Among 64 queried DEGs, 48 genes were recognized by the STRING database. C-X-C motif chemokine ligand 8 (CXCL8), intercellular adhesion molecule 1 (ICAM1), Melanoma growth-stimulatory activity/growth-regulated protein α (CXCL1), vascular cell adhesion molecule 1 (VCAM-1), and nerve growth factor (NGF) were introduced as hub nodes.

Conclusion: Findings indicate that inflammation is the main initial target of LDIR at the cellular level which is associated with alteration in the other essential functions of the irradiated cells.

Keywords: Radiation; Gene expression; Inflammation; Network analysis; Central node.

Introduction

The effect of long-term low-dose ionizing radiation (LDIR) on the radiated cells indicates that the immune system is the target of radiation.[1] Investigations have revealed that chronic low-dose γ-radiation induces cytokine profile change in irradiated mice.[2] Several other biological effects of chronic low-dose of ionizing radiation are reported by researchers.[3] Proteomics as a high throughput method is applied to study the biological effects of chronic LDIR. Based on the literature, the glycolysis pathway and pyruvate dehydrogenase availability are inhibited by low and moderate radiation doses in the liver of the radiated mice. Another effect is significant long-term alterations in lipid metabolism in the liver of the tested animals.[4,5]

Genomics is used to detect the molecular mechanism of chronic LDIR. Based on genomics findings, dissimilar appearances of LDIR-induced cellular responses may have diverse signal transduction pathways.[6] Like proteomics and genomics, bioinformatics is a method that is applied to investigate the molecular mechanism after radiation and LDIR on the different types of tested biological samples.[7,8] Network analysis is a method that is useful to identify the significant differentially expressed genes (DEGs) or differentially expressed proteins (DEPs). Several gene profiles and also protein profiles after radiation are analyzed via network analysis.[9,10]

Please cite this article as follows: Ansari M, Rezaei-Tavirani M, Hamzeloo-Moghadam M, Razzaghi M, Arjmand B, Zamanian Azodi M, et al. Investigation into chronic low-dose ionizing radiation effect on gene expression profile of human HUVECs cells. *J Lasers Med Sci.* 2022;13:e35. doi:10.34172/jlms.2022.35.

Protein-protein interaction (PPI) network analysis is a method which is based on interactions between a set of genes or proteins that may construct a network. Since the properties of elements of the network are not similar, the importance of each node may differ from the other nodes to form the network. The crucial nodes in the network are known as central nodes. One critical central node is a hub node. A hub node is connected to most nodes of the studied network.[11,12]

In the present study, gene expression profiles of human umbilical vein endothelial cells (HUVECs) in the absence and presence of 4.66 mGy/h for 6 hours by using cesium-137 were downloaded from Gene Expression Omnibus (GEO), and the significant DEGs were determined to find the crucial dysregulated genes among large numbers of DEGs. The identified significant DEGs were screened via PPI network analysis to introduce the limited numbers of DEGs that were targeted by LDIR and induced the main alteration in the function of the radiated cells.

Methods

Data of GSE66720 that is related to the cultured HUVECs was downloaded from GEO (https://www.ncbi.nlm.nih.gov/geo/query/acc.cgi?acc=gse66720). The cells were synchronized in G1 cell cycle phase. Four gene expression profiles in GSE66720 which are characterized as GSM1630524 and GSM1630531 relative to the gene expression profiles of the control cells and GSM1630530 and GSM1630537 of the cells that were exposed to 4.66 mGy/h for 6 hours by using cesium-137 were selected to be analyzed.

The gene expression profiles were analyzed by using GEO2R to match the sample statistically via volcano plot, meandiff plot, expression plot, and box plot. The dysregulated genes that were characterized by FC > 1.5 and *P* value < 0.05 were selected as the significant DEGs.

The significant DEGs were imported in Cytoscape software[13] via the "protein query" of the STRING database to construct a PPI network. The queried DEGs were connected to each other via undirected edges. Since most of the queried DEGs were isolated, 70 first neighbors were added to the DEGs from the STRING database and the main connected component of the formed network was analyzed by the "NetworkAnalyzer" application of Cytoscape. Four centrality parameters including degree value, betweenness centrality, closeness centrality, and stress were determined for the nodes of the main connected component. Five top nodes among the queried DEGs based on the degree value were identified as queried DEGs hubs. Similarly, five first neighbors' hubs were introduced. The biological roles of the hub nodes were searched and discussed to find a new perspective on chronic ionizing radiation effects on the cultured cells.

Results

As it is shown in Figure 1, volcano plot analysis revealed that the gene expression profiles of the treated cells versus the control cells are significantly discriminated. A considerable number of the genes are significantly up-regulated and down-regulated. Considering -0.6 > log2FC > 0.6 which refers to fold change (FC) > 1.5, distribution of log2expression of the significant DEGs is presented in Figure 2. As it is depicted in Figure 3,

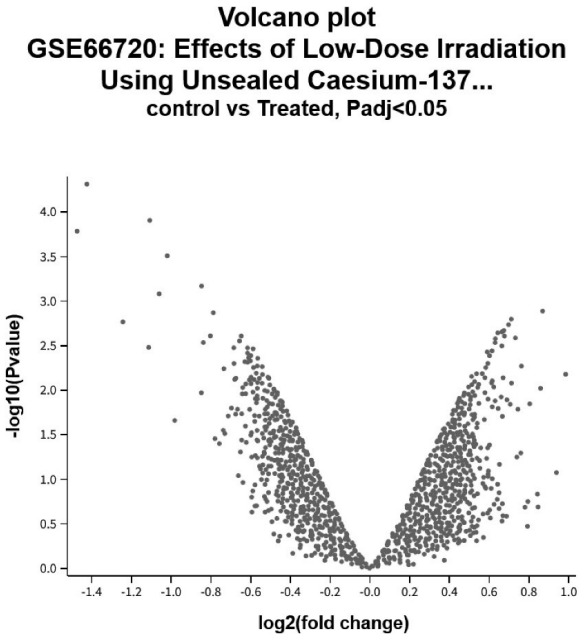

Figure 1. Volcano Plot, Representation of -log10(*P* Value) Versus log2FC for Gene Expression Profiles of the Radiated Cells Relative to the Control Cells. *P*-adjective < 0.05 was considered

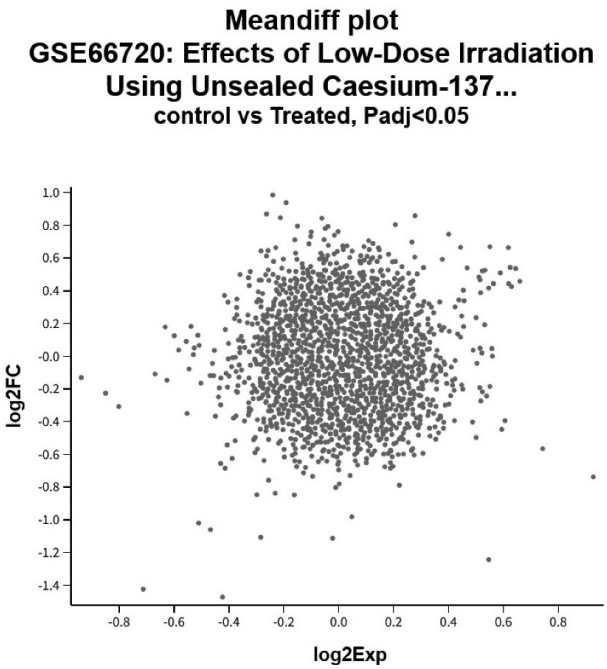

Figure 2. Meandiff Plot, Representation of log2FC Versus log2 Expression for Gene Expression Profiles of the Radiated Cells Relative to the Control Cells. *P*-adjective < 0.05 was considered

the gene expression profiles of the control cells and the radiated cell are comparable. The distribution boxes are central median and the frequency of the expressed points is limited to nearly equal ranges. Based on the curves in Figure 4, the density of the genes with zero intensity is the maximum and the dysregulated genes are characterized by fewer values of density. The curves in Figure 4 are similar and comparable, but they are not unique based on the types of proteins. A list of 64 significant DEGs is presented in Table 1. 25 upregulated DEGs versus 39 downregulated individuals are introduced.

Among the 64 introduced DEGs, 48 individuals were recognized by the STRING database and the network was constructed by Cytoscape software (see Figure 5). Only 27% of the 48 recognized DEGs including 13 genes were included in the main connected component by 27 connections. When 70 first neighbors were added to the 48 queried DEGs, the main connected component including 70 first neighbors and 34 queried DEGs (equal to 71% of the queried DEGs) was formed by 2729 links between the nodes. The main connected component which is constructed from first neighbors and the related queried DEGs is shown in Figure 6. The nodes of the network are laid out based on the degree value.

Results of the main connected component including four centrality parameters such as degree value, betweenness centrality (BC), closeness centrality (CC), and stress are tabulated in Table 2. The 5 top queried hubs and also 5 top first neighbor hubs are determined and shown in Table 3.

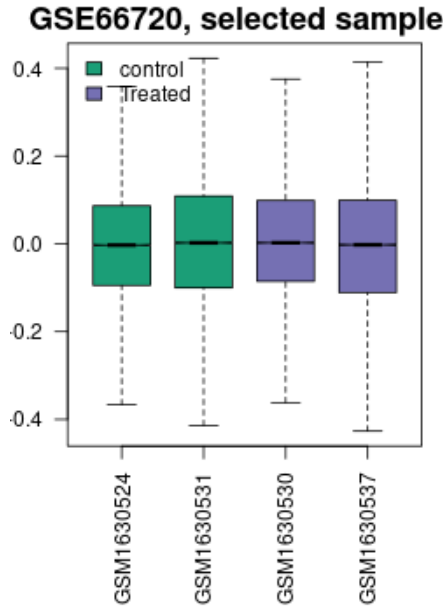

Figure 3. Box Plot Representation of Expression Distribution for Gene Expression Profiles of the Two Radiated Cell Samples Relative to the Control Cells. Four quarters are shown for each gene expression profile

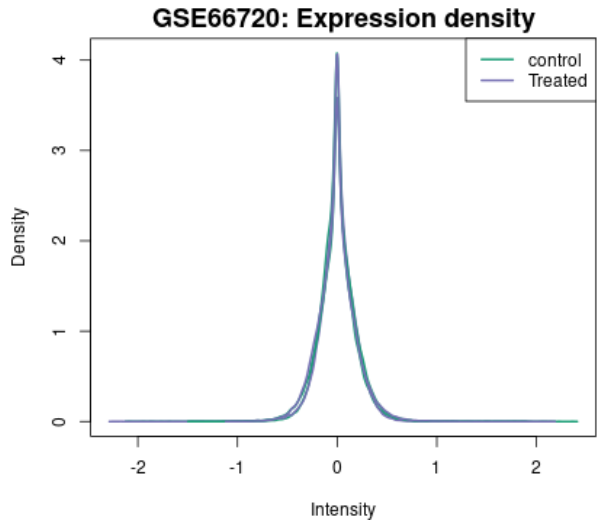

Figure 4. Expression Plot Representation of Density Versus Intensity of Expression for Four Gene Expression Profiles of the Radiated Cell Samples Relative to the Control Cells

Discussion

Network analysis as a useful method is applied to describe the molecular mechanism due to radiation at the cellular level.[14] Here, the gene expression alteration of HUVECs after radiation of 4.66 mGy/h for 6 hours by using cesium-137 was studied via PPI network analysis. Results from Figures 1-4 indicate that there are significant DEGs that discriminate the radiated cells from the controls. As it is depicted in Table 1, 64 significant DEGs were selected to be analyzed. In the first step of the analysis, 16 DEGs were not included for more investigation because they were not recognized in the STRING database.

As it is shown in Figure 5, the recognized DEGs cannot form an informative PPI network and there are a weak number of connections between the studied DEGs. Adding proper numbers of the first neighbors to the queried DEGs is a suitable method that leads to the construction of an appropriate PPI network for investigation.[15] The network including the recognized DEGs and added individuals is shown in Figure 6. Analysis of the constructed network led to the introduction of 5 queried DEGs as hubs and also five hub nodes among the added first neighbors. However, the other centrality parameters such as betweenness centrality, closeness centrality, and stress for the hub nodes were significant. As shown in Table 3, all first neighbor hubs are characterized by a higher value of degree relative to the DEGs hubs.

AKT1, ACTB, GAPDH, IL6, and TNF are the first neighbor hubs, while the queried DEGs hubs are CXCL8, ICAM1, CXCL1, VCAM1, and NGF. The role of AKT1 in the radiated sample is investigated by several researchers. As it is reported, AKT1 plays a role in the suppression of apoptosis in the radiated germ cells in vivo. Activation of AKT1 and radiosensitivity have been investigated to show the role of this gene in DNA double-strand break repair.[16,17] Both ACTB and GAPDH are considered control genes in radiotherapy investigation.[18] Inducing

Table 1. List of 64 significant DEGs which discriminate the radiated cells from the controls

Gene Title	Gene Symbol	LogFC	*P* Value
Cytochrome P450 family 1 subfamily A member 1	CYP1A1	-1.473	0.00
Vascular cell adhesion molecule 1	VCAM1	-1.424	0.00
Phospholipase A2 group IVC	PLA2G4C	-1.243	0.00
Intercellular adhesion molecule 1	ICAM1	-1.113	0.00
Histone deacetylase 9	HDAC9	-1.107	0.00
Selectin E	SELE	-1.06	0.00
Cerebellin 2 precursor	CBLN2	-1.02	0.00
Myozenin 2	MYOZ2	-0.848	0.01
C-X-C motif chemokine ligand 8	CXCL8	-0.847	0.00
F-box protein 32	FBXO32	-0.838	0.00
Intercellular adhesion molecule 1	ICAM1	-0.803	0.00
Interleukin 4 induced 1	IL4I1	-0.735	0.01
G-patch domain containing 2 like	GPATCH2L	-0.713	0.02
PDZ and LIM domain 5	PDLIM5	-0.685	0.00
Neural precursor cell expressed, developmentally down-regulated 4-like, E3 ubiquitin protein ligase	NEDD4L	-0.684	0.01
CD274 molecule	CD274	-0.68	0.01
Rho GTPase activating protein 6	ARHGAP6	-0.676	0.01
Nerve growth factor	NGF	-0.675	0.02
Retinol dehydrogenase 13	RDH13	-0.674	0.01
Nuclear paraspeckle assembly transcript 1 (non-protein coding)	NEAT1	-0.666	0.02
NFKB inhibitor zeta	NFKBIZ	-0.656	0.00
Microtubule associated protein 2	MAP2	-0.651	0.01
Glycerophosphocholine phosphodiesterase 1	GPCPD1	-0.647	0.00
TOLLIP antisense RNA 1 (head to head)	TOLLIP-AS1	-0.645	0.02
Myozenin 2	MYOZ2	-0.642	0.01
SPOC domain containing 1	SPOCD1	-0.64	0.01
PDZ and LIM domain 5	PDLIM5	-0.638	0.01
Small integral membrane protein 10 like 2B///small integral membrane protein 10 like 2A	SMIM10L2B///SMIM10L2A	-0.625	0.01
Exosome component 7///C-type lectin domain family 3 member B	EXOSC7///CLEC3B	-0.624	0.01
Sulfotransferase family 1C member 4	SULT1C4	-0.616	0.00
C-X-C motif chemokine ligand 1	CXCL1	-0.616	0.00
Apoptosis associated transcript in bladder cancer	AATBC	-0.607	0.00
Peptidoglycan recognition protein 1	PGLYRP1	-0.606	0.01
Transmembrane p24 trafficking protein 10	TMED10	-0.605	0.02
Neuronal PAS domain protein 2	NPAS2	-0.604	0.01
cAMP responsive element binding protein 5	CREB5	-0.602	0.00
Neural precursor cell expressed, developmentally down-regulated 4-like, E3 ubiquitin protein ligase	NEDD4L	-0.601	0.00
Carnitine O-octanoyltransferase	CROT	0.612	0.01
Zinc fingers and homeoboxes 3	ZHX3	0.614	0.00
FOXF1 adjacent non-coding developmental regulatory RNA	FENDRR	0.615	0.01
Neuronal growth regulator 1	NEGR1	0.615	0.02
Angiopoietin 2	ANGPT2	0.623	0.01
Sphingosine-1-phosphate receptor 3	S1PR3	0.63	0.00
S-phase kinase-associated protein 2, E3 ubiquitin protein ligase	SKP2	0.63	0.01
Homeobox A11	HOXA11	0.631	0.00
Ecotropic viral integration site 2B	EVI2B	0.643	0.00
TLR4 interactor with leucine rich repeats	TRIL	0.645	0.02
Fanconi anemia complementation group A	FANCA	0.66	0.01
Coxsackie virus and adenovirus receptor	CXADR	0.663	0.00

Table 1. Continued

Gene Title	Gene Symbol	LogFC	*P* Value
BBSome interacting protein 1	BBIP1	0.67	0.01
Angiopoietin 2	ANGPT2	0.674	0.00
Syntrophin beta 2	SNTB2	0.674	0.01
TLR4 interactor with leucine rich repeats	TRIL	0.677	0.00
TIMP metallopeptidase inhibitor 3	TIMP3	0.698	0.00
Centrosomal protein 350	CEP350	0.706	0.01
Mannosidase alpha class 1C member 1	MAN1C1	0.711	0.00
Zinc finger CCCH-type containing 11A	ZC3H11A	0.712	0.01
Lipase E, hormone sensitive type	LIPE	0.732	0.00
Pleckstrin and Sec7 domain containing 3	PSD3	0.762	0.01
ATP2A1 antisense RNA 1	ATP2A1-AS1	0.804	0.01
Coxsackie virus and adenovirus receptor	CXADR	0.858	0.01
Nuclear receptor subfamily 1 group D member 2	NR1D2	0.985	0.01

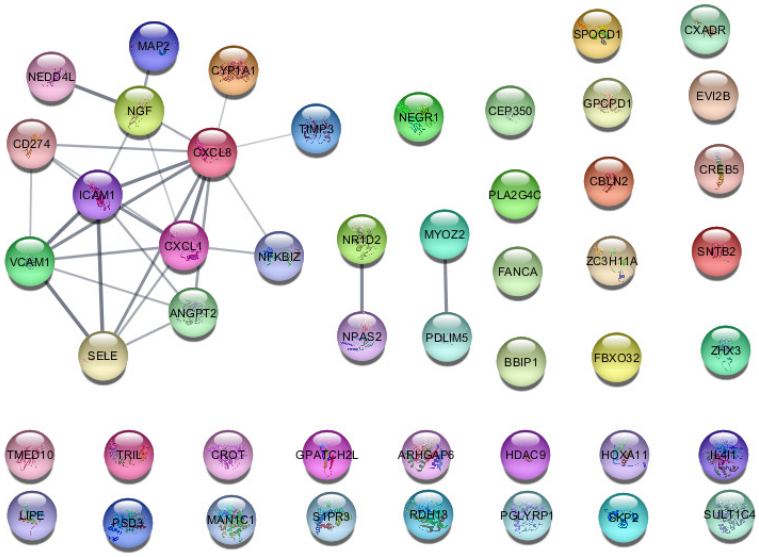

Figure 5. The 48 Recognized DEGs Including 31 Isolated Genes, 4 Paired Genes, and a Main Connected Component. The 13 nodes of the main connected component are connected to each other by 27 edges

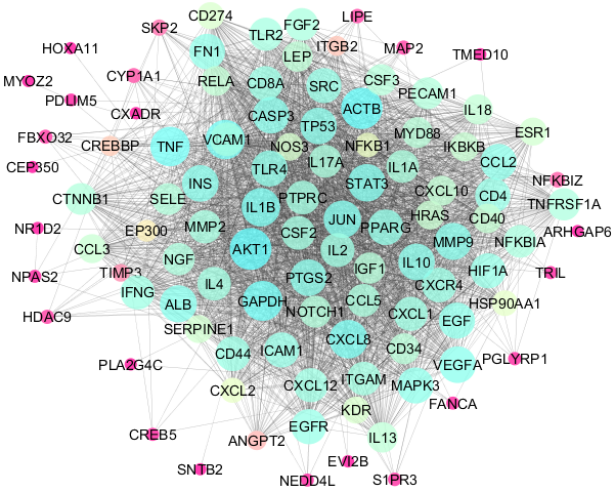

Figure 6. The main connected component including 104 nodes and 2729 links is presented and the related nodes are laid out by the degree value

the expression of IL6 by ionizing radiation in the human fibroblasts is a well-studied subject by researchers.[19] The role of TNF-α in the modulation of cell responses to ionizing radiation is discussed in a study by Pal et al.[20]

C-X-C motif chemokine ligand 8 (CXCL8) which is known as IL8 is involved in the tumor microenvironment. As it is reported by investigators, CXCL8 initiates leucocyte infiltration and neovascularization, which precedes invasion and metastasis in tumor progression.[21] Intercellular adhesion molecule 1 (ICAM1) is responsible for several immune functions such as response to inflammatory mediators and different stimuli.[22] Melanoma growth-stimulatory activity/growth-regulated protein α (CXCL1) is an important player in angiogenesis, inflammation, tumorigenesis, and wound healing processes.[23] Investigations indicate that silencing of vascular cell adhesion molecule 1 (VCAM-1) leads to

Table 2. The 104 Nodes of the Main Connected Component and the Relative Central Parameters

No.	Display Name	Query Term	Degree	Betweenness Centrality	Closeness Centrality	Stress
1	AKT1		87	0.043	0.866	3496
2	ACTB		86	0.040	0.858	3232
3	GAPDH		83	0.013	0.831	2366
4	IL6		82	0.010	0.824	2166
5	TNF		82	0.010	0.824	2166
6	CXCL8	CXCL8	80	0.006	0.811	1796
7	IL1B		80	0.006	0.811	1796
8	JUN		78	0.010	0.798	1638
9	STAT3		78	0.016	0.805	1776
10	ALB		77	0.007	0.780	1406
11	MMP9		77	0.006	0.780	1362
12	CASP3		76	0.006	0.780	1268
13	IL10		76	0.006	0.774	1232
14	INS		76	0.018	0.780	1862
15	PTGS2		76	0.012	0.780	1520
16	TP53		76	0.010	0.786	1668
17	VEGFA		76	0.003	0.786	1196
18	CCL2		75	0.003	0.763	1006
19	EGF		75	0.004	0.774	1228
20	MAPK3		75	0.020	0.780	1898
21	TLR4		75	0.010	0.769	1634
22	FN1		74	0.006	0.763	1194
23	PPARG		74	0.012	0.774	1776
24	CD4		73	0.002	0.757	800
25	EGFR		73	0.007	0.769	1414
26	HIF1A		73	0.005	0.769	1218
27	ICAM1	ICAM1	73	0.002	0.757	756
28	SRC		73	0.007	0.769	1428
29	CD44		72	0.002	0.757	886
30	CD8A		72	0.002	0.752	778
31	CXCR4		72	0.004	0.752	890
32	CXCL1	CXCL1	71	0.002	0.736	744
33	CXCL12		71	0.002	0.746	746
34	IFNG		71	0.001	0.746	600
35	IL2		71	0.001	0.741	592
36	CSF2		70	0.001	0.741	614
37	IL4		70	0.001	0.736	494
38	ITGAM		70	0.001	0.736	558
39	PTPRC		70	0.015	0.736	1522
40	VCAM1	VCAM1	70	0.001	0.736	616
41	MMP2		69	0.021	0.736	2140
42	TLR2		69	0.005	0.736	1038
43	CCL5		68	0.001	0.720	440
44	FGF2		68	0.003	0.736	880
45	IL17A		68	0.002	0.725	612
46	IL1A		68	0.003	0.725	776
47	NFKBIA		68	0.010	0.741	1620
48	NGF	NGF	67	0.005	0.725	782
49	TNFRSF1A		67	0.004	0.715	762
50	CTNNB1		66	0.005	0.730	1018
51	NOTCH1		66	0.010	0.730	1314
52	PECAM1		66	0.001	0.720	532

Table 2. Continued

No.	Display Name	Query Term	Degree	Betweenness Centrality	Closeness Centrality	Stress
53	SELE	SELE	66	0.001	0.720	624
54	CSF3		65	0.001	0.705	392
55	IGF1		65	0.003	0.715	612
56	CD34		64	0.001	0.710	392
57	MYD88		64	0.004	0.705	902
58	IL13		63	0.001	0.696	282
59	LEP		63	0.003	0.710	720
60	CXCL10		62	0.000	0.691	260
61	IL18		62	0.000	0.691	258
62	RELA		62	0.003	0.701	838
63	CD40		61	0.002	0.687	530
64	CCL3		60	0.000	0.682	228
65	HRAS		60	0.022	0.701	2828
66	IKBKB		60	0.008	0.696	1242
67	ESR1		58	0.006	0.691	1000
68	SERPINE1		58	0.006	0.682	868
69	NOS3		57	0.022	0.682	2874
70	CD274	CD274	56	0.000	0.660	234
71	KDR		56	0.003	0.673	462
72	HSP90AA1		53	0.018	0.665	1372
73	CXCL2		52	0.001	0.636	194
74	NFKB1		51	0.002	0.648	566
75	EP300		44	0.025	0.624	3588
76	CREBBP		37	0.025	0.595	3380
77	ITGB2		36	0.005	0.579	524
78	ANGPT2	ANGPT2	33	0.000	0.572	56
79	TIMP3	TIMP3	25	0.000	0.545	4
80	SKP2	SKP2	19	0.000	0.534	8
81	NFKBIZ	NFKBIZ	16	0.000	0.500	4
82	CYP1A1	CYP1A1	14	0.000	0.512	18
83	LIPE	LIPE	11	0.000	0.505	0
84	HDAC9	HDAC9	10	0.000	0.502	0
85	MAP2	MAP2	10	0.000	0.495	0
86	FBXO32	FBXO32	9	0.000	0.495	0
87	S1PR3	S1PR3	7	0.000	0.488	2
88	PGLYRP1	PGLYRP1	6	0.000	0.462	0
89	CREB5	CREB5	5	0.000	0.488	0
90	FANCA	FANCA	5	0.000	0.484	0
91	NEDD4L	NEDD4L	5	0.000	0.481	2
92	NPAS2	NPAS2	5	0.001	0.464	156
93	TRIL	TRIL	5	0.000	0.460	0
94	PDLIM5	PDLIM5	4	0.019	0.484	644
95	CXADR	CXADR	2	0.000	0.470	0
96	EVI2B	EVI2B	2	0.000	0.435	0
97	NR1D2	NR1D2	2	0.000	0.389	0
98	PLA2G4C	PLA2G4C	2	0.000	0.452	0
99	TMED10	TMED10	2	0.000	0.456	0
100	ARHGAP6	ARHGAP6	1	0.000	0.414	0
101	CEP350	CEP350	1	0.000	0.375	0
102	HOXA11	HOXA11	1	0.000	0.426	0
103	MYOZ2	MYOZ2	1	0.000	0.327	0
104	SNTB2	SNTB2	1	0.000	0.407	0

Table 3. The 5 Top Added First Neighbor Hubs and 5 Top Queried DEGs Hubs

No.	Display Name	Query Term	Degree	Betweenness Centrality	Closeness Centrality	Stress
1	AKT1		87	0.043	0.866	3496
2	ACTB		86	0.040	0.858	3232
3	GAPDH		83	0.013	0.831	2366
4	IL6		82	0.010	0.824	2166
5	TNF		82	0.010	0.824	2166
6	CXCL8	CXCL8	80	0.006	0.811	1796
7	ICAM1	ICAM1	73	0.002	0.757	756
8	CXCL1	CXCL1	71	0.002	0.736	744
9	VCAM1	VCAM1	70	0.001	0.736	616
10	NGF	NGF	67	0.005	0.725	782

Note. The nodes are picked based on the degree value.

inflammation and apoptosis inhibition.[24] As it is reported, nerve growth factor (NGF) is associated with several processes such as differentiation, proliferation, protection, and survival of peripheral sensory and sympathetic neurons. This gene plays a crucial role in the translation of various environmental stimuli into pathological and physiological feedback. It is shown that NGF levels are related to stressful events.[25] When the five queried hubs (CXCL8, ICAM1, CXCL1, VCAM1, and NGF) are investigated together, a document about the progression of oral squamous cell carcinoma appears, reflecting the tumorigenesis property of the applied radiation.[26]

Findings indicate that the main target of chronic ionizing radiation is the activation of the inflammatory system which can lead to the initiation of related processes such as apoptosis, cell differentiation and proliferation, angiogenesis, invasion and metastasis in tumor progression. An investigation indicated that chronic low-dose-rate ionizing radiation induced the upregulation of the genes against oxidative stress in the human fibroblast cells.[27]

Conclusion

It can be concluded that the targets of chronic low-dose-rate ionizing radiation are different genes; however, the genes related to the inflammatory system are the crucial ones. It seems the inflammatory system is the main gate of damages that end in tumorigenesis and metastasis.

Acknowledgment

Shahid Beheshti University of Medical Sciences supported this research.

Conflicts of Interest

All authors declare they have no conflicts of interest.

Ethical Considerations

This project was approved by Shahid Beheshti University of Medical Sciences (No. IR.SBMU.RETECH.REC.1400.889).

References

1. Lumniczky K, Impens N, Armengol G, Candéias S, Georgakilas AG, Hornhardt S, et al. Low dose ionizing radiation effects on the immune system. Environment international. 2021;149:106212.
2. Shin SC, Lee K-M, Kang YM, Kim K, Kim CS, Yang KH, et al. Alteration of cytokine profiles in mice exposed to chronic low-dose ionizing radiation. Biochemical and biophysical research communications. 2010;397(4):644-9.
3. Chaudhry MA, Omaruddin RA, Kreger B, De Toledo SM, Azzam EI. Micro RNA responses to chronic or acute exposures to low dose ionizing radiation. Molecular biology reports. 2012;39(7):7549-58.
4. Leszczynski D. Radiation proteomics: a brief overview. Proteomics. 2014;14(4-5):481-8.
5. Bakshi MV, Azimzadeh O, Barjaktarovic Z, Kempf SJ, Merl-Pham J, Hauck SM, et al. Total body exposure to low-dose ionizing radiation induces long-term alterations to the liver proteome of neonatally exposed mice. Journal of proteome research. 2015;14(1):366-73.
6. Tang FR, Loke WK. Molecular mechanisms of low dose ionizing radiation-induced hormesis, adaptive responses, radioresistance, bystander effects, and genomic instability. International journal of radiation biology. 2015;91(1):13-27.
7. Perez-Gelvez YNC, Camus AC, Bridger R, Wells L, Rhodes Jr OE, Bergmann CW. Effects of chronic exposure to low levels of IR on Medaka (Oryzias latipes): a proteomic and bioinformatic approach. International Journal of Radiation Biology. 2021;97(10):1485-501.
8. Bakshi MV, Barjaktarovic Z, Azimzadeh O, Kempf SJ, Merl J, Hauck SM, et al. Long-term effects of acute low-dose ionizing radiation on the neonatal mouse heart: a proteomic study. Radiation and environmental biophysics. 2013;52(4):451-61.
9. Sekaran TSG, Kedilaya VR, Kumari SN, Shetty P, Gollapalli P. Exploring the differentially expressed genes in human lymphocytes upon response to ionizing radiation: a network biology approach. Radiation oncology journal. 2021;39(1):48.
10. Moore R, Puniya BL, Powers R, Guda C, Bayles KW, Berkowitz DB, et al. Integrative network analyses of transcriptomics data reveal potential drug targets for acute radiation syndrome. Scientific reports. 2021;11(1):1-14.
11. Vella D, Marini S, Vitali F, Di Silvestre D, Mauri G, Bellazzi R. MTGO: PPI network analysis via topological and functional module identification. Scientific reports. 2018;8(1):1-13.
12. Athanasios A, Charalampos V, Vasileios T. Protein-protein interaction (PPI) network: recent advances in drug discovery. Current drug metabolism. 2017;18(1):5-10.
13. Zamanian-Azodi M, Arjmand B, Razzaghi M, Tavirani MR, Ahmadzadeh A, Rostaminejad M. Platelet and haemostasis

are the main targets in severe cases of COVID-19 infection; a system biology study. Archives of Academic Emergency Medicine. 2021;9(1).
14. Yu D, Li Y, Ming Z, Wang H, Dong Z, Qiu L, et al. Comprehensive circular RNA expression profile in radiation-treated HeLa cells and analysis of radioresistance-related circRNAs. PeerJ. 2018;6:e5011.
15. Rezaei Tavirani M, Arjmand B, Razzaghi M, Ahmadzadeh A. 50S Ribosomal proteins family is the main target of cinnamon extract: a network analysis. Research Journal of Pharmacognosy. 2021;8(2):63-8.
16. Rasoulpour T, DiPalma K, Kolvek B, Hixon M. Akt1 suppresses radiation-induced germ cell apoptosis in vivo. Endocrinology. 2006;147(9):4213-21.
17. Oeck S, Al-Refae K, Riffkin H, Wiel G, Handrick R, Klein D, et al. Activating Akt1 mutations alter DNA double strand break repair and radiosensitivity. Scientific reports. 2017;7(1):1-11.
18. Saligan L, Hsiao C, Wang D, Wang X, John LS, Kaushal A, et al. Upregulation of α-synuclein during localized radiation therapy signals the association of cancer-related fatigue with the activation of inflammatory and neuroprotective pathways. Brain, behavior, and immunity. 2013;27:63-70.
19. Brach M, Gruss H, Kaisho T, Asano Y, Hirano T, Herrmann F. Ionizing radiation induces expression of interleukin 6 by human fibroblasts involving activation of nuclear factor-kappa B. Journal of Biological Chemistry. 1993;268(12):8466-72.
20. Pal S, Yadav P, Sainis K, Shankar BS. TNF-α and IGF-1 differentially modulate ionizing radiation responses of lung cancer cell lines. Cytokine. 2018;101:89-98.
21. Gales D, Clark C, Manne U, Samuel T. The chemokine CXCL8 in carcinogenesis and drug response. International Scholarly Research Notices. 2013;2013.
22. Singh M, Thakur M, Mishra M, Yadav M, Vibhuti R, Menon AM, et al. Gene regulation of intracellular adhesion molecule-1 (ICAM-1): A molecule with multiple functions. Immunology Letters. 2021;240:123-36.
23. Dhawan P, Richmond A. Role of CXCL1 in tumorigenesis of melanoma. Journal of leukocyte biology. 2002;72(1):9-18.
24. Jiang L, Yang A, Li X, Liu K, Tan J. Down-regulation of VCAM-1 in bone mesenchymal stem cells reduces inflammatory responses and apoptosis to improve cardiac function in rat with myocardial infarction. International Immunopharmacology. 2021;101:108180.
25. Ceci FM, Ferraguti G, Petrella C, Greco A, Tirassa P, Iannitelli A, et al. Nerve growth factor, stress and diseases. Current Medicinal Chemistry. 2021;28(15):2943-59.
26. Shan Q, Takabatake K, Omori H, Kawai H, Oo MW, Nakano K, et al. Stromal cells in the tumor microenvironment promote the progression of oral squamous cell carcinoma. International journal of oncology. 2021;59(3):1-17.
27. Loseva O, Shubbar E, Haghdoost S, Evers B, Helleday T, Harms-Ringdahl M. Chronic low dose rate ionizing radiation exposure induces premature senescence in human fibroblasts that correlates with up regulation of proteins involved in protection against oxidative stress. Proteomes. 2014;2(3):341-62.